Structural Eng./Earthquake Eng., JSCE, Vol. 15, No. 1, 115s—125s, 1998 April

A STUDY ON WIND RESISTANT DESIGN OF LONG-SPAN BRIDGES BASED ON FIELD OBSERVATION RESULT

Hiroshi KATSUCHI [1], Kazuo TADA [2] and Makoto KITAGAWA [3]

[1] Member of JSCE, M. S., Planning & Development Department, Honshu-Shikoku Bridge Authority (1-22, Onoedori 4, Chuo-ku, Kobe 651-0088)

[2] Master of Eng., Executive Director, Yachiyo Engineering Corporation (4-70, Shiromi 1, Chuo-ku, Osaka, 540-0001)

[3] Member of JSCE, Master of Eng., General Manager of Tarumi Construction Office Honshu-Shikoku Bridge Authority, (1-66, Hiraiso 1, Tarumi-ku, Kobe 655-0892)

In wind-resistant design of long-span bridges, their behavior against the wind is evaluated through wind tunnel testing or analytical approaches. Little evidence has been reported so far as to whether or not the wind characteristics acting on bridges are the same as assumed in the design code and they behave in the same way as assumed in it. This paper presents the results of a study on the validity of wind-resistant design for long-span bridges based on field observation results of the Ohnaruto Bridge and the Minami Bisan-Seto Bridge. The possibility that the wind load for long-span bridges could be reduced is suggested by reconsidering the spatial correlation of the wind.

Key Words: *field observation, gust response, long-span bridge, spatial correlation, wind-resistant design*

1. INTRODUCTION

In wind-resistant design of long-span bridges, what is done first is modeling of the wind characteristics to be applied to the structures, then estimating and evaluating the response, and finally judging whether or not the response is within allowable limits. The detailed procedure is provided in the Wind-Resistant Design Code for the Honshu-Shikoku Bridges (1976), etc. [1)-3)].

Since the wind characteristics are considerably affected by the topographical conditions around a bridge site, a suitable model of them is chosen from examples statistically classified according to region and topography [4)], or identified by wind observation data at the site [2)]. Regarding the estimation and evaluation of the response, a wind tunnel test and/or an analytical method can be used. Wind tunnel testing which investigates aeroelastic phenomena of a scaled bridge model set in a wind tunnel has primarily been used so far. The analytical method computes the response by modeling the wind characteristics and applying them to the bridge. Examples of the analytical method are a buffeting analysis which is used as the procedure for wind-resistant design [2)], a flutter analysis [5)-8)], and a numerical simulation for aeroelastic phenomena, the so-called numerical wind tunnel [9)], the latter dependent on remarkable computer development.

There do not exist many reports which check the validity of the wind-resistant design of long-span bridges based on field observation data. Checking the validity could yield important data for making the wind-resistant design more accurate. For this reason, anemometers, optical displacement gauges and accelerometers are installed on some of the Honshu-Shikoku Bridges. Inputs to, and output from, the bridges, that is, wind characteristics and bridge responses have been recorded automatically and for a long time when strong wind strikes the bridges.

This paper describes results bearing on the validity of the existing wind-resistant design method, as reflected in both field observation data and analytical studies. The field observation data used here were collected on the Ohnaruto Bridge (a three-span truss-stiffened suspension bridge with a main span of 876 m) and the Minami Bisan-Seto Bridge (a three- span truss-stiffened suspension bridge with a main span of 1100 m) during typhoon No.19 in September, 1991 (referred to hereafter as the 9119 typhoon) and typhoon No.13 in September,1993

This paper is translated into English from the Japanese paper, which originally appeared on J. Struct. Mech. Earthquake Eng., JSCE, No.543/ I-36, pp.163–173, 1996.7.

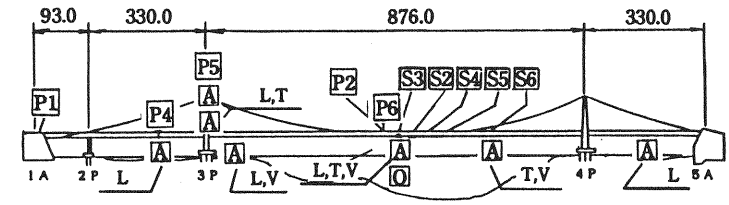

(1) Ohnaruto Bridge

[Legend]
A: Accelerometer (L: longitudinal, T: transverse, V: vertical)
D: Displacement Gauge
AD: Accel.-Displacement Gauge
O: Optical Displacement Gauge
P: Wind-Mill Anemometer
S3, S4, S6: Sonic Anemometer
S2, S5: Aerovane

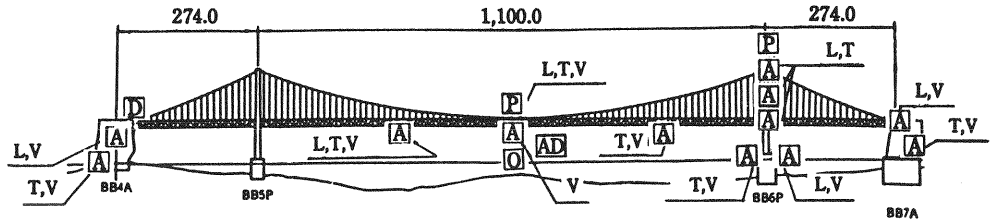

(2) Minami Bisan-Seto Bridge (unit: m)

Fig.1 Arrangements of instruments for data acquisition system

(referred to hereafter as the 9313 typhoon). Since it was confirmed that both bridges have sufficient stability for flutter, and that they do not excite vortex shedding according to the field observation data as well as the wind tunnel testing at design stages, their buffeting response is mainly studied here in this research.

This paper is translated into English from the Japanese paper, which originally appeared on J. Struct. Mech. Earthquake Eng., JSCE, No.543/ I-36, pp.163–173, 1996.7.

2. OUTLINE OF FIELD OBSERVATION

Fig. 1 depicts arrangements of instruments for data acquisition for the Ohnaruto Bridge and the Minami Bisan-Seto Bridge. Since the Ohnaruto Bridge is expected to experience the strongest wind among the Honshu-Shikoku Bridges (reference wind speed at 10m above sea level is 50 m/s for a 150-year return period), emphasis was placed on observing wind characteristics. Therefore, several sonic anemometers were located longitudinally on the deck for the purpose of measuring the spatial correlation of the wind. For the purpose of measuring bridge responses, accelerometers were installed at important points and an optical displacement gauge was used at a center point of the deck span to measure static displacement and very long periodic response more accurately.

The field observation systems were designed so that data acquisition started automatically when the wind speed exceeded a set level (usually 20 m/s in a 10-minute mean wind speed), and the data were recorded for the following 10 minutes with a sampling time interval of 50 msec on magnetic tape.

3. WIND CHARACTERISTICS ACTING ON THE BRIDGES

(1) Wind Speed and Turbulence Intensity

Fig. 2 and **Table 1** outline the wind characteristics observed on the Ohnaruto Bridge and the Minami Bisan-Seto Bridge during the 9119 and 9313 typhoons. The maximum mean wind speed and the maximum wind speed at the Ohnaruto Bridge were 40.4 m/s and 54.1 m/s, respectively while for the Minami Bisan-Seto Bridge they were 35.4 m/s and 42.0 m/s, respectively.

The gust factor, which is the ratio of the maximum wind speed to the mean wind speed, ranges approximately from 1.2 to 1.3. As for the longitudinal turbulence intensity, I_u which is proportional to the gust factor, almost all recorded values lie between 6% and 12 %. Although several of those observed on the Minami Bisan-Seto Bridge exceeded 15 %, these are thought to be affected by the structure, particularly by the main cables and the hanger cables because they were recorded for large skewed winds.

Based on the results above, about 10 sets of the data (10 minute per set) for each typhoon and bridge, which have conditions of high wind speed and nearly normal wind, were selected from all the data in order to analyze the characteristics in detail.

(2) Turbulence Scale

The turbulence scales were analyzed for the data

Table 1 Wind characteristics analyzed in this study

	Ohnaruto Br.		Minami Bisan-Seto Br.	
Date	9/27, 1991	9/3-4, 1993	9/27, 1991	9/3-4, 1993
Time	13:24-23:24	22:17-4:07	21:57-0:48	15:54-4:30
No. of Data	51×10min.	29×10min.	6×10min.	24×10min.
Max. Speed (m/s)	20.8 – 54.1	27.3 – 47.1	23.6 – 42.0	17.0 – 35.6
Ave. Speed (m/s)	14.9 – 40.4	21.7 – 37.3	19.2 – 35.4	12.3 – 29.8
Turbulence Intensity: I_u (%)	5.3 – 12.0	6.2 – 10.4	6.8 – 10.3	5.7 – 20.9 *)
Anemometer	Sonic type **)		Wind-mill type	
Elevation of Anemometer	71.0 m		100.8 m	
Distance from Typhoon	300 km	100 km	200 km	50 km

*) Large turbulence was observed in wind along bridge axis.
**) Spatial correlation was analyzed using sonic anemometers' data.

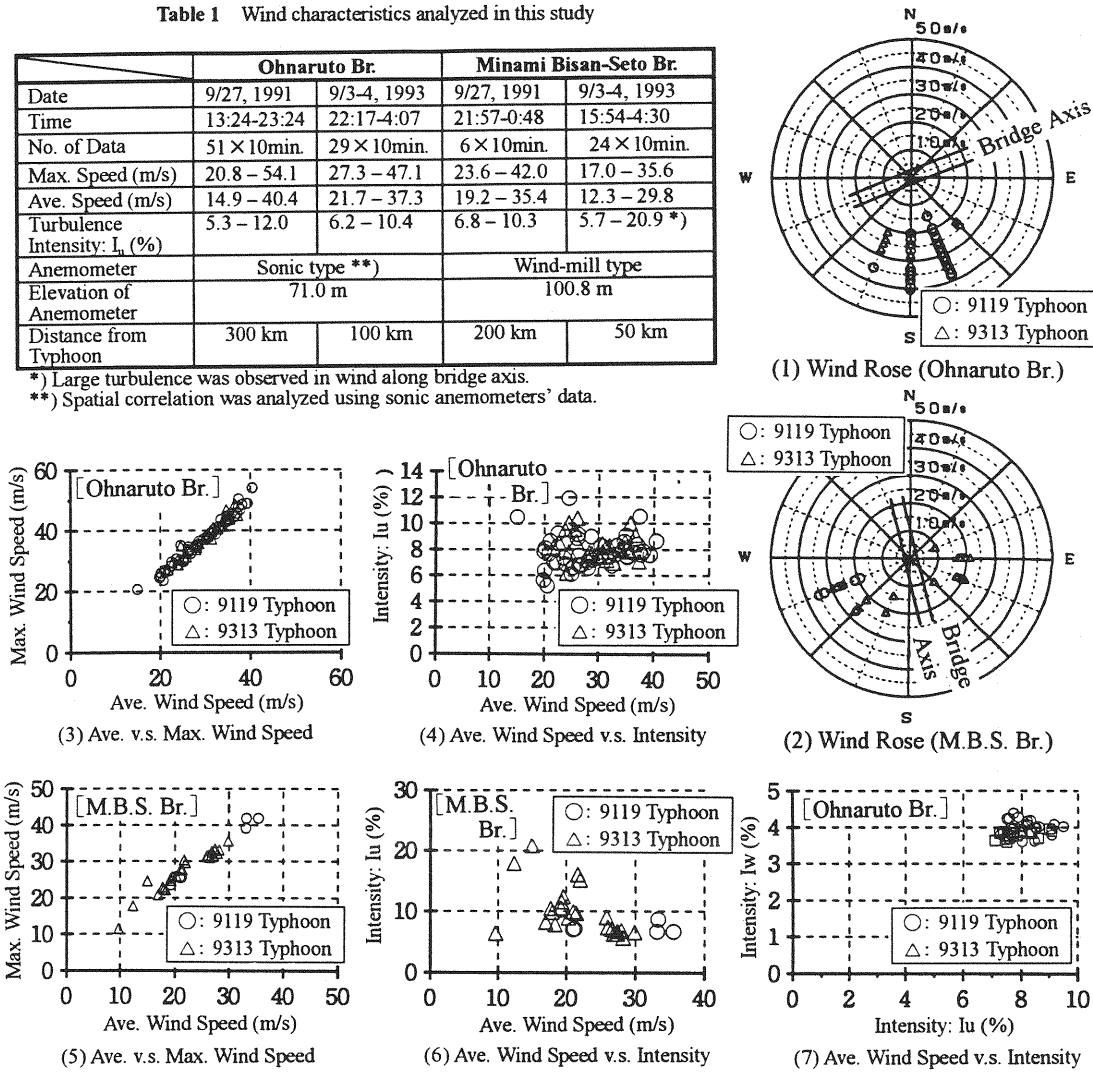

Fig. 2 Wind speed and turbulence intensity on Ohnaruto Bridge and Minami Bisan-Seto Bridge

observed on the Ohnaruto Bridge. The data were collected by two sonic anemometers (S3 and S4) and two vane anemometers (S2 and S5). A calculation of the turbulence scale was performed by three methods, [1] integrating an auto-correlation coefficient to the point where the lag time becomes zero, [2] deriving it from the power spectrum at zero frequency, and [3] deriving it from the frequency at which the power spectrum reaches its peak [10]. The longitudinal turbulence scale of longitudinal velocity fluctuation, L_u^x was evaluated as the mean value among the three methods, while the longitudinal turbulence scales of vertical velocity fluctuation, L_w^x were evaluated by the third method. On the other hand, the transverse turbulence scales of longitudinal and vertical velocity fluctuations, L_u^y and L_w^y were calculated by cross-correlation coefficients between the two points (S3 - S4 and S2 - S5) [10].

Fig. 3 depicts the turbulence scales on the Ohnaruto Bridge. The L_u^x ranges from 100 m to 300 m. Although L_u^x values were also analyzed using the data from a wind-mill type anemometer on the Minami Bisan-Seto Bridge, they ranged from 130 m to 320 m, which are similar in magnitude to those on the Ohnaruto Bridge. Analyzing the L_u^x by the three methods mentioned above revealed that L_u^x values by the second and third method were in good agreement while that by the first method tended to give relatively large values. The average coefficient of variation of L_u^x was 0.16 except for a few cases analyzed by the first method in which the auto-

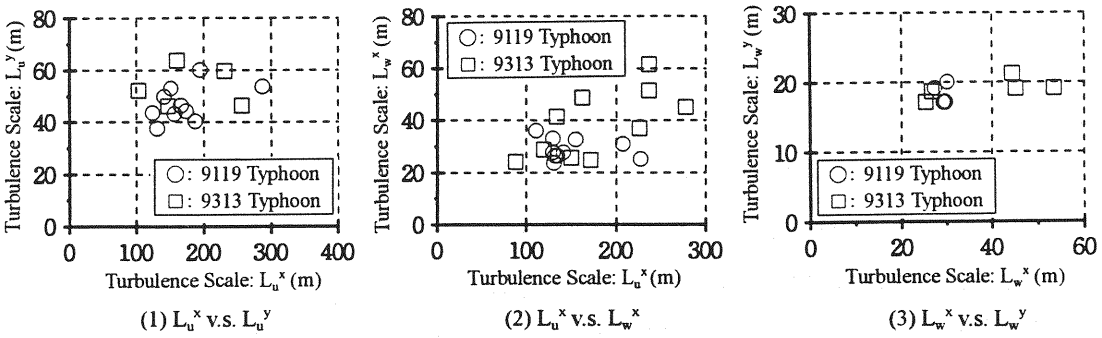

Fig.3 Turbulence scale on Ohnaruto Bridge

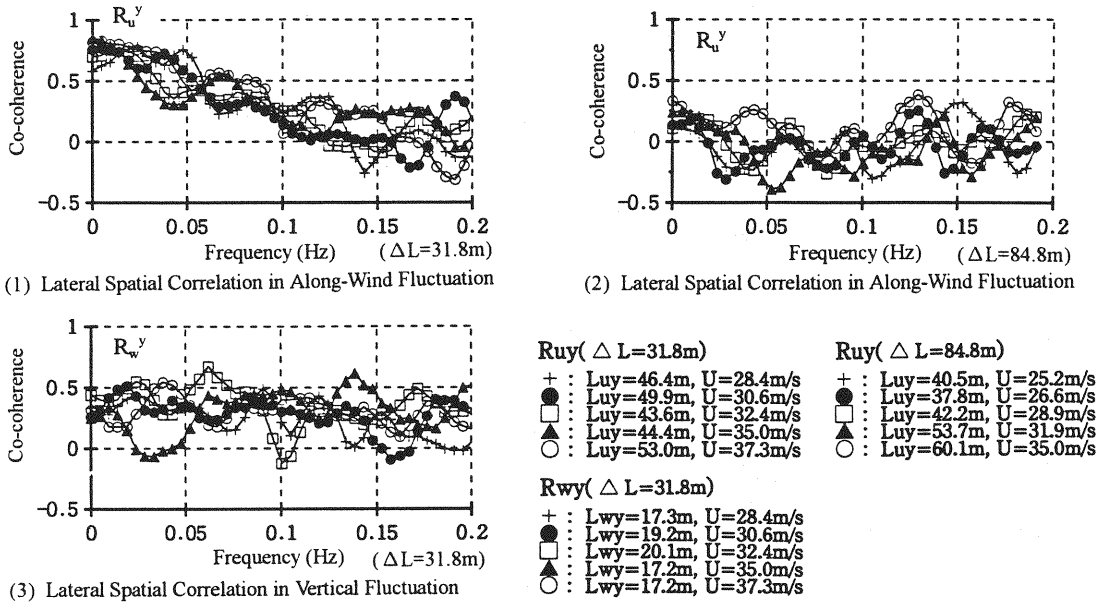

Fig.4 Spatial correlation on Ohnaruto Bridge at 9119 typhoon

correlation coefficient failed to cross the zero.

The values of L_u^y ranged from 40 m to 60 m; and the ratio of L_u^y to L_u^x ranged from 1/2 to 1/5.5. This is nearly the same range as found by Shiotani et al. [11]. They showed that L_u^y / L_u^x ranged from 1/2.5 to 1/4 for the data measured at Satoura, where the fetch is a flat region that faces the sea. They also showed the same result for the turbulence scale of the vertical velocity fluctuation. L_w^y / L_w^x of the Ohnaruto Bridge which also ranged from 1/1.5 to 1/3, corresponding to their result.

The ratios of the turbulence scale of the vertical and longitudinal velocity fluctuation, L_w^x / L_u^x were also analyzed by them, which ranged from 1/4 to 1/5. Those of the Onaruto Bridge show similar results, ranging from 1/3 to 1/9.

(3) Spatial Correlation

spatial correlation of the wind fluctuation along the bridge deck was analyzed by using the data measured on the Ohnaruto Bridge during the 9119 typhoon. The data used here are those measured by the S3 and S4 sonic anemometers (separation distance ΔL = 31.8 m) and by the S2 and S5 vane anemometers (distance ΔL = 84.8 m). The transverse spatial correlation of the longitudinal and vertical velocity fluctuation were analyzed here. The spatial correlation was evaluated as co-coherence which was given by the real part of the cross

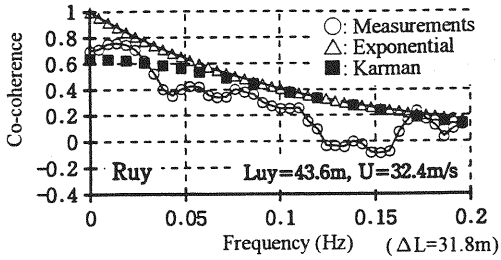

(1) Lateral Spatial Correlation in Along-Wind Fluctuation

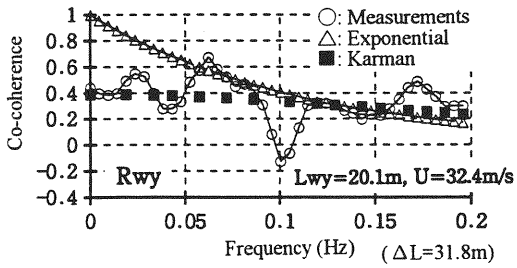

(3) Lateral Spatial Correlation in Vertical Fluctuation

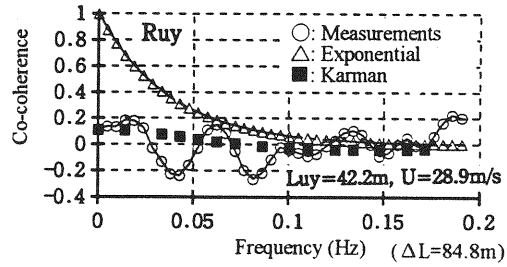

(2) Lateral Spatial Correlation in Along-Wind Fluctuation

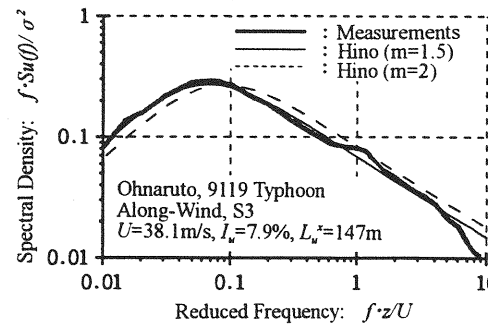

Fig.5 Comparisons of spatial correlation between measurements and theories (Ohnaruto Bridge, 9119 typhoon)

Fig.6 PSD of along-wind fluctuation (Ohnaruto Bridge, 9119 typhoon)

spectrum. **Fig. 4** shows the results for the five cases analyzed here. It is noted that the correlation decreases as the frequency becomes high, and that it is lower than unity at zero frequency. In addition, it becomes strong for the larger distance cases. It can also be seen that the correlation becomes large as the turbulence scale becomes large. The reason that the values of the co-coherence fluctuate around zero beyond the zero crossing may be that measurement and analytical errors are relatively larger than the cross- spectrum in that region.

For one of the cases above, the measured value was compared with the exponential type function used in the Design Code (Eq. 1) and the functions derived from the von Karman type cross spectrum (referred to as Karman type function hereafter) proposed by Harris [12] and Roberts&Surry [13] (Eqs. 2 and 3).

[Exponential type function]

$$R_u^y \text{ or } R_w^y = \exp(-k\frac{f\Delta L}{U}) \qquad (1)$$

[Karman type function]

$$R_u^y = \frac{2^{1/6}}{\Gamma(5/6)}\eta^{5/6}K_{5/6}(\eta) - \frac{\eta^{11/6}}{2}K_{1/6}(\eta) \qquad (2)$$

$$R_w^y = \frac{2^{1/6}}{\Gamma(5/6)}\eta^{5/6}K_{5/6}(\eta) - \frac{\eta^{11/6}K_{1/6}(\eta)}{1+188.7\left(fL_w^y/U\right)^2} \qquad (3)$$

with

$$\eta = \frac{0.7468\Delta L}{L_u^y \text{ or } L_w^y}\sqrt{1+70.78\left[\frac{f(L_u^y \text{ or } L_w^y)}{U}\right]^2}$$

where R_u^y and R_w^y are respectively transverse spatial correlation of the longitudinal and vertical velocity fluctuation, k is a decay factor, f is frequency, ΔL is the distance between two points, U is the mean wind speed, Γ is a Gamma function, K is a second modified Bessel function, and L_u^y and L_w^y are respectively transverse turbulence scales of the longitudinal and vertical velocity fluctuation.

From **Fig. 5**, it can be seen that the Karman type function is a better expression than the exponential type function with respect to agreement in the low frequency region and the fact that the correlation is lower than unity at zero frequency. This might be a reason why the Karman type function can better express actual turbulence structure through taking the turbulence scale into the function. That is, since the actual turbulence structure is three-dimensional, the correlation is lower than unity at zero frequency due to the three dimensional characteristics of turbulence vortices in the case of long separation distance, particularly longer than the turbulence scale. This can also be said for a smaller turbulence scale as it can be understood by comparing **Fig. 3** with **Fig. 4**.

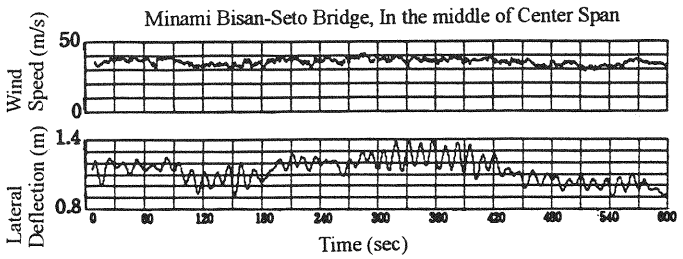

Fig.7 Time history of wind speed and lateral deck deflection (Minami Bisan-Seto Bridge, 9119 typhoon)

(4) Wind Spectra

Wind power spectra of the longitudinal velocity fluctuation were analyzed by using the sonic anemometer data observed on the Ohnaruto Bridge during the 9119 typhoon as shown in **Fig. 6**. The Wind-Resistant Design Code for the Honshu-Shikoku Bridges provides that the Hino spectrum be used for the longitudinal direction. **Fig. 6** also shows the comparison between the Hino spectrum and the measurement. The Hino spectrum is defined by

$$S_u(f) = 0.476 \frac{u^2}{\beta} \left\{ 1 + \left(\frac{f}{\beta} \right)^2 \right\}^{-5/6} \qquad (4)$$

with

$$\beta = 1.169 \times 10^{-3} \frac{U_{10}\alpha}{\sqrt{K_r}} \left(\frac{z}{10} \right)^{(2m\alpha - 1)}$$

where $S_u(f)$ is the power spectrum density of the longitudinal velocity fluctuation, u^2 is the variance of the longitudinal velocity fluctuation, U_{10} is a reference speed, α is a power of the wind speed profile, z is elevation, m is a modifying coefficient and K_r is a surface friction coefficient.

The measurement is in good agreement in the case where m = 1.5 in Eq. 4; however, m = 2 is used in the design code. This can be understood from the fact that the turbulence scale, L_u^x is obtained by the equation $L_u^x = 0.119 \times U/B$, which in turn is derived by integrating the auto- correlation function of Eq. 4 with respect to the time, yielding 144 m for m = 1.5, wheres the measured scale is 147 m. For m = 2 in Eq. 4, L_u^x is 109 m and the spectrum peak shifts to higher frequency. But it is possible that m = 2 will be the most suitable value because L_u^x on the Ohnaruto bridge ranges from 100 to 300 m as shown in **Fig.3**. Since the turbulence scale is not included in Eq. 4, it is important to choose the modifying coefficient properly instead, and it is also suggested that some variation in this should be taken into account in designing.

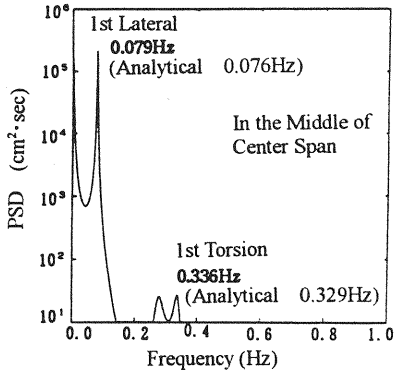

(1) PSD of Lateral Deflection

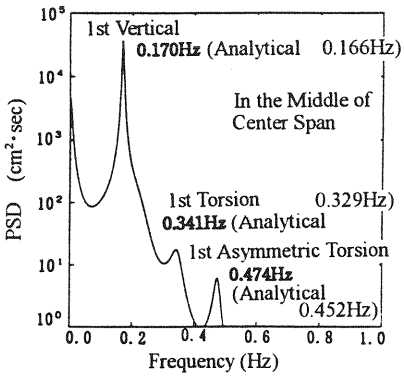

(2) PSD of Vertical Deflection

Fig.8 PSD of deck deflection (Minami Bisan-Seto Bridge, 9119 typhoon)

4. CHARACTERISTICS OF BRIDGE RESPONSE TO THE WIND

(1) Time History and Power Spectra of Response

Fig. 7 shows one of the time history responses in the middle of the center span of the girder of the Minami Bisan-Seto Bridge during the 9119 thphoon,and it also shows wind speed records.

Analyzing the wind data shows that the mean speed was 35.4 m/s, the maximum speed was 42.0 m/s, the gust factor is 1.19 and the longitudinal turbulence intensity, I_u is 6.8 %. As for the bridge response, static lateral deflection was 1.13 m and the maximum dynamic response was 0.26 m. Long periodic variation in the response of the girder might be due to long periodic wind speed fluctuation because they appear to correspond to each other.

Fig. 8 shows the power spectrum of the response of the girder as obtained by a maximum entropy method. It can be seen that primarily fundamental modes contribute to the power in both lateral and vertical directions.

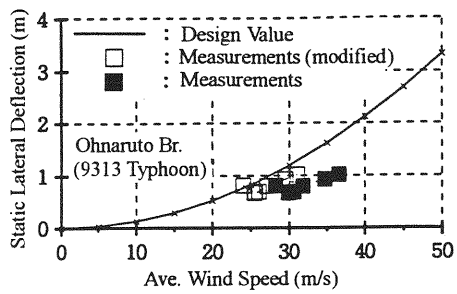

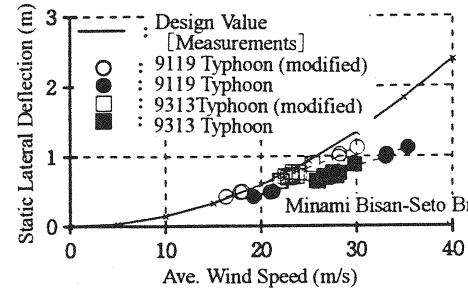

Fig.9 Relationship between wind speed and static deflection of deck

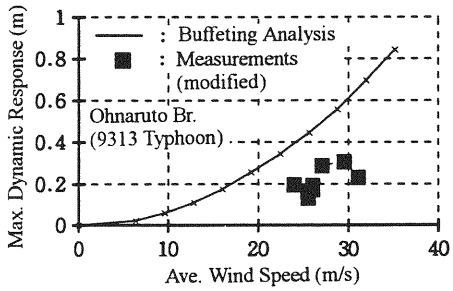

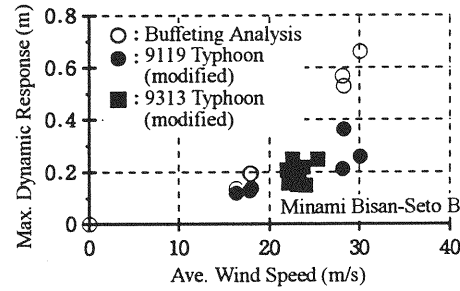

Fig.10 Relationship between wind speed and dynamic response of deck

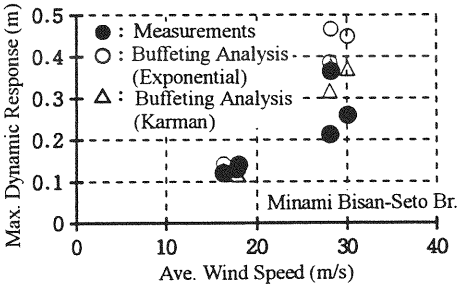

Fig.11 Comparison of max. dynamic response between measurements and buffeting analysis

(2) Relationship between Lateral Static Displacement and Wind Speed

Fig. 9 show the static displacement (● and ■) of the Ohnaruto and Minami Bisan-Seto Bridges vs. the wind speed. The static displacement measured are 30% - 40% lower than the design values which are shown by the solid lines. The authors confirmed that the lateral static displacement measured in a full-model wind-tunnel test of the Akashi-Kaikyo and Tatara bridges are in good agreement by less than 5% error with those analyzed by suitable models and methods [14]. Therefore, the errors between the measurements and design values were thought to be caused by improper analytical conditions and/or methods. Also, two factors to be investigated were noted here. One is the difference between the elevation of the anemometer (71 m above the sea) and the mean elevation of the girder which is used in designing (54.3 m above the sea). Assuming the power law of 1/7 for the wind profile which is the design value, approximately 4% higher wind speed should be observed at the elevation of the anemometer. The other is that the anemometer may indicate a wind speed higher than that of the oncoming flow due to an influence of the girder.

The previous study [15] showed that 10% - 15% higher wind speed were observed at the anemometer on a girder, but that this trend depended on the location of the anemometer and the wind direction. Based on these two reasons, it was judged that the anemometer indicated 15-percent higher wind speed against the oncoming flow at the mean elevation of the girder. Finally, the measured static displacements were plotted again with the wind speeds reduced to 85% (O and □ in **Fig. 9**). It can be seen that the resulting measurements are in good agreement with the design values. Therefore, analysis of data and computations hereafter will be performed with the mean wind speed which reduced to 85% for both Ohnaruto and Minami Bisan-Seto Bridges.

(3) Study of Dynamic Response

Fig. 10 shows the relationships between the dynamic responses of the girders and the wind speeds of the Ohnaruto and Minami Bisan-Seto Bridges. The solid line and white circles in the figures represent the corresponding buffeting analyses. The buffeting analysis used here is a frequency domain analysis [2] in which the response power spectra are computed using wind power spectra, aerodynamic admittance, joint mode acceptances and mechanical admittance functions as shown in Eq. 5.

$$S_m(\omega) = \sum_{k=1}^{mode} \phi_{km}^2 \frac{|H_k(\omega)|^2}{\omega_k^4} \sum_{i=1}^{node} \sum_{j=1}^{node} \phi_{ki}\phi_{kj} \times \left|\chi_{ij}(\omega)\right|^2 F_i F_j S_{ij}(\omega) \quad (5)$$

where ω is a circular frequency, ω_k is a k^{th} mode circular natural frequency, ϕ_{km} is a value of the k^{th} modal deformation at the m node, $|H_k(\omega)|^2/\omega_k^4$ is the mechanical admittance function of the k^{th} mode, $|\chi_{ij}(\omega)|^2$ is an aerodynamic admittance function, F_i and F_j are buffeting forces based on the quasi-steady theory at the i and j nodes and $S_{ij}(\omega)$ is a wind cross-spectrum at the i and j nodes.

The measurements are considerably smaller than the computed values. Since the analyses were performed with a longitudinal turbulence intensity of 0.1 which is a design value, the measurements observed in the turbulence intensity of less than 0.1 should be below than the analyses. In the analyses, the log decrement value of structural damping for the first lateral mode was assumed to be 0.06. Because the log decrement damping including aerodynamic damping was identified as 0.16 from buffeting response data of the Minami Bisan-Seto Bridge at 30 m/s by using a random decrement method [16], and the aerodynamic damping was calculated as 0.1. by the quasi-steady theory.

As mentioned in 3.(3), since the Karman type function is more appropriate than the exponential type one for the expression of the spatial correlation, the buffeting analysis was performed using the Karman type function. **Fig. 11** shows the comparisons of the buffeting responses calculated by using both types of functions for the Minami Bisan-Seto Bridge at the 9119 typhoon. In these analyses, the turbulence intensities were adjusted to the observed values. The cases using the Karman type function show that the dynamic responses reduce by about 20% and that use of the Karman type function yields better estimations compared with the exponential type function. The reason that differences persist between the measurements and analyses even though the Karman type function is used is that other factors were present that were not considered in the analysis, for example, aero-dynamic admittance [17], coupling of modes [18), 19)], etc. These were not pursued further in this study.

5. EXAMINING THE VALIDITY OF THE WIND-RESISTANT DESIGN FOR LONG-SPAN BRIDGES

(1) Wind-resistant design for buffeting

In the wind-resistant design of long-span bridges, effects of the buffeting which is caused by wind turbulence are taken into account by multiplying a wind load due to mean wind speed by a modification factor (refer to Eq. 6). The modification factor is decided upon based on the result of the buffeting analysis with the wind characteristics specified in the design code and with a specific structure. In the Wind-Resistant Design Code for the Honshu-Shikoku Bridges, the modification factors are categorized in advance based on the results of buffeting analyses with specified wind characteristics and for typical suspension bridges having different span lengths [1]. For the Akashi-Kaikyo Bridge, the Tatara Bridge and the Kurushima Bridges, buffeting analyses were performed individually, and the modification factors were chosen for reasonable design [2), 3)].

$$P_D = \mu \frac{\rho U_z^2}{2} C_D A_n \quad (6)$$

where P_D is a design wind load, μ is a modification factor resulting from wind speed fluctuation, U_z is the design wind speed, C_D is a drag coefficient and A_n is a projection area.

(2) Examination of the validity of design conditions

As mentioned in the introduction, buffeting is considered an aeroelastic phenomena here, and the validity of the current wind-resistant design method for long-span bridges is examined in terms of the formulation of wind characteristics and the estimation of bridge responses.

a) Wind characteristics (turbulence intensity)

As turbulence intensity generally decreases with elevation, the Wind-Resistant Design Code for the Honshu-Shikoku Bridges stipulates the relationship between longitudinal turbulence intensity, I_u and elevation, z based on the formulation by Davenport [10] (see Eq. (7)). For the Akashi-Kaikyo Bridge, the relationship is determined in Eq. (8) based on the measurement at the observation tower near the bridge site. The vertical turbulence intensity, I_w is taken as $0.5I_u$.

$$I_u = 0.1225\left(\frac{z}{10}\right)^{-\alpha} \quad (7)$$

Table 2 Parameters of bridges in buffeting analysis

	Minami Bisan-Seto Br.	3rd Kuru-shima Br.	Akashi-Kaikyo Br.	2500m-Box Br.	2500m-Truss Br.
Center Span	1,100 m	1,030 m	1,990 m	2,500 m	2,500 m
1st Lateral Mode	0.076 Hz	0.068 Hz	0.038 Hz	0.034 Hz	0.033 Hz
1st Vertical Mode	0.166 Hz	0.158 Hz	0.064 Hz	0.056 Hz	0.053 Hz
1st Torsion Mode	0.329 Hz	0.367 Hz	0.140 Hz	0.151 Hz	0.133 Hz
Design Wind Speed	58 m/s	53 m/s	60 m/s	65 m/s	66 m/s
Power in Wind Profile	1/7	1/7	1/8	1/8	1/8
Decay Factor	7	8	8	8	8
L_u^y, L_u^z	(Turbulence Scale)		60 m		
L_w^y, L_w^z	(Turbulence Scale)		40 m		
No. of Modes	100 modes in Lateral, and 200 modes in Vertical and Torsion are used.				

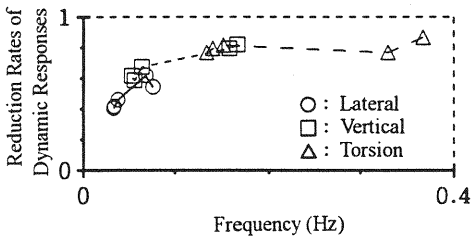

Fig.12 Reduction ratio of response (Max. deflection)

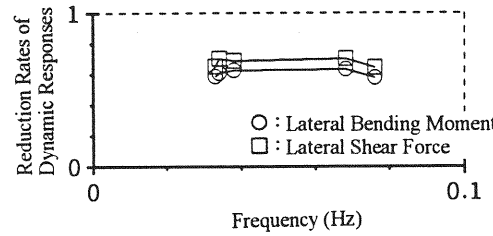

Fig.13 Reduction ratio of response (Lateral moment & shear force)

$$I_u = 0.130\left(\frac{z}{10}\right)^{-\alpha} \quad (8)$$

Both equations approximately give the value of I_u to be 0.1 for the girders of the Honshu-Shikoku Bridges whose mean deck elevations are 50 m to 80 m. The turbulence intensities I_u ranging from 0.06 to 0.12 measured in this study are approximately the same as 0.1. As for the vertical turbulence intensity I_w, the measured values are about half as large as I_u. From this point of view, the assumption of turbulence intensity in the current design code can be judged to be reasonable.

b) Wind characteristics (spatial correlation and turbulence scale)

From the results in 3.(3), it was found that the Karman type function is more suitable than the exponential type for the expression of spatial correlation, particularly in the low frequency range. In particular, since the frequency of the first natural mode of long-span bridges, which is the dominant contribution to buffeting response, decreases to this low frequency region, it is very important that spatial correlation should be evaluated with greater accuracy. In addition, the design force in some members of long-span bridges such as the chords of the truss stiffened girder of the Akashi-Kaikyo Bridge and the tower base of the Tatara Bridge are subject to the wind load. Buffeting response in design is expected to reduce if the Karman type function is used. Therefore, it is thought that the accurate formulation of spatial correlation will improve the rationality of the wind-resistant design.

c) Wind characteristics (power spectra)

There are some proposed functions for the power spectrual density of the longitudinal wind velocity fluctuation such as the Hino spectrum (which is used for the Honshu-Shikoku Bridges), and the Karman, Harris and Davenport functions [10]. The power spectrual density in the high frequency region is theoretically proportional to a -5/3 power of wave number, as shown in Eq. (4). From **Fig. 6**, the measured spectrum is also approximately proportional to the same number. Therefore, it is thought that the power spectrual density function in the current design is reasonable in terms of its shape. However the peak frequency of the density cannot be fixed, and a standard power spectrum cannot be determined because the measured turbulence scales vary. From this point of view, it is important that the variation of the peak frequency of the power spectrum due to the variation of the turbulence scale should be taken into account.

d) Characteristics of bridge responses (design wind load)

The design wind loads on bridges are calculated by multiplying the wind load due to a mean wind speed by the modification factor obtained from a buffeting analysis, as shown in Eq. (6). As mentioned above, it was found that the Karman type function is more accurate than the exponential type function for the spatial correlation of wind. Considering the

buffeting response of long-span bridges, since low frequency natural modes exist in the low frequency region where the difference of the spatial correlation between the two functions becomes large, there must exist an effect of this on the buffeting response.

In order to investigate the effects of the difference in the spatial correlation functions, buffeting analyses in the frequency domain, the theory of which was described above, were performed [20]. The analyses were done for five bridges as shown in **Table 2** and with design conditions for each bridge. For the cases using the Karman type function for the spatial correlation, the transverse turbulence scales of the longitudinal and vertical velocity fluctuation, L_u^y and L_w^y were assumed to be 60 m and 40 m, respectively by referring to the measurements on the Ohnaruto Bridge.

Fig. 12 shows reduction-rates of dynamic parts of the lateral, vertical and torsional responses when the spatial correlation function was changed from the exponential type to the Karman type. The abscissa of each point represents the lowest natural frequencies for each direction: lateral, vertical and torsion because contribution of the lowest mode to total response is the most dominant. From the figure, it can be seen that the rate of reduction decreases as the frequency reduces for all the directions. The reason may be due to the fact that the correlation by the Karman type is less than unity at zero frequency and is always smaller than that by the exponential type, which trend becomes significant as the frequency reduces.

In addition, **Fig. 13** also shows the rates of reduction of the lateral bending moments and shear forces of the decks, plotted by the same method in **Fig. 12**. The change of the reduction rates with frequency is seen to be less significant; however these reduce throughout the range, which is different from the case of displacement. This may be due to the fact that high frequency modes contribute to the lateral bending moment and shear force, and that the reduction effects of the low frequency modes are diminished, thus the dependency on frequency did not appear significantly.

However the wind loads on long-span bridges are calculated in such a manner that the wind load associated with mean wind speed is multiplied by the gust factor for the lateral bending moment and lateral shear force, which is obtained by a buffeting analysis as described before. The gust factor of a buffeting analysis decreases in the case of using the Karman type correlation function, which is more suitable for natural wind. This results in reducing the design wind load; therefore, the possibilities of a more rational wind-resistant design for long-span bridges are suggested.

6. CONCLUDING REMARKS

The study on the wind-resistant design for long-span bridges was performed based on the field observation results of the Ohnaruto and Minami Bisan-Seto Bridges during the 9119 and 9313 typhoons. The results obtained from the study are as follows:

(1) The current wind-resistant design method was verified with respect to turbulence intensity and power spectra. But since the characteristics of natural wind vary widely, it is suggested that a structure should be checked for cases in which the wind characteristics vary from the design value.

(2) It was confirmed that the spatial correlation function derived from the cross spectrum expression based on the von Karman spectrum (Karman type function) is a more appropriate expression of spatial correlation than the exponential type function used in the current wind- resistant design, particularly in the low-frequency region.

(3) The effects of the spatial correlation of wind velocity on the bridge response, particularly the buffeting response, were investigated by comparing the measurements with the buffeting analysis. Consequently, the analysis with the Karman type correlation function was in better agreement with the measured response. It can be said that using the Karman type function is more rational than using the current exponential one in the wind-resistant design for long-span bridges.

(4) It was also found that there is a possibility that using the Karman type function can reduce the wind load in the current wind-resistant design. This is thought to lead the design of the structure of long-span bridges which may be subject to the wind load to being rational.

REFERENCES

1) Honshu-Shikoku Bridge Authority: *Wind-Resistant Design Code for the Honshu-Shikoku Bridges (1976)*, 1976.
2) Honshu-Shikoku Bridge Authority: *Wind-Resistant Design Manual for the Akashi-Kikyo Bridge*, 1990.
3) Honshu-Shikoku Bridge Authority: *Wind-Resistant Design Code for Bridges of the Onomichi-Imabari Route*, 1994.
4) Japan Road Association: *Wind-Resistant Design Manual for Road Bridges*, 1991.
5) Scanlan, R. H.: "The Action of Flexible Bridges under Wind, I: Flutter Theory", *Journal of Sound and Vibration*, 60(2), pp. 187-199, 1978.
6) Fujino, Y., Iwamoto, M., Ito, M., Hikami, Y., Takeda, K, Miyata, T. and Tatsumi, M.: "Full-Model Wind Tunnel Testing of Very Long-Span Suspension Bridge with Box Girder", *Journal of JAWE*, Vol. 46, pp. 1-17, 1991.
7) Tanaka, H., Yamamura, N. and Shiraishi, N.: "Multi-Mode Flutter Analysis and Two & Three Dimensional Model

Tests on Bridges with Non-Analogous Modal Shapes", *Proc. of JSCE*, Vol. 10, No. 2, pp. 71s-82s, 1993.
8) Katsuchi, H., Miyata, T., Kitagawa, M., Sato, H. and Hikami, Y.: "A Study on Coupled Flutter in Wind Tunnel Testing of the Akashi-Kaikyo Bridge", *Proc. of 13th Symposium of JAWE*, pp. 383-388, 1994.
9) Okajima, A.: "Present and Future of Numerical Wind Tunnel Testing in Wind Engineering", *Bridge and Foundation*, Vol. 23, No. 8, pp. 94-102, 1989.
10) Okauchi, I., Ito, M. and Miyata, T.: *Wind-Resistant Structure*, Maruzen, pp. 65-74, 1977.
11) Shiotani, M.: *Characteristics of Strong Wind*, Kaihatsu-Sha, 1992.
12) Harris, R. I.: "Proc. of the Seminar on Modern Design of Wind Sensitive Structures", *Institution of Civil Engineers*, 1970.
13) Roberts, J. B. and Surry, D.: "Coherence of Grid-Generated Turbulence", *Journal of the Engineering Mechanics Division*, pp. 1227-1245, 1973.
14) Katsuchi, H., Miyata, T., Yasuda, M., Yokoyama, K. and Yamada, H.: "A Study on Static Deflection due to Wind Loading of Long-Span Suspension Bridge", *Proc. of 12th Symposium of JAWE*, pp. 333-338, 1992.
15) Honshu-Shikoku Bridge Authority: *Report on Field Observation of the Hitsuishi-Jima Bridge under Construction*, 1988.
16) Tamura, Y., Sasaki, A., Sato, T. and Kohsaka, R.: "Evaluation of Damping of Structure in Strong Wind by RD Method", *Proc. of 12th Symposium of JAWE*, pp. 303-308, 1992.
17) Sato, H., Matsuno, H. and Kitagawa, M.: "Measuring of Aerodynamic Admittance of the Akashi-Kaikyo Bridge", *Proc. of 13th Symposium of JAWE*, pp. 131-136, 1994.
18) Miyata, T., Yamada, H., Boonyapinyo, V. and Santos J. C.: "Three-Dimensional Buffeting Response Analysis of Long-Span Bridges by A Time Domain Approach", *Proc. of 13th Symposium of JAWE*, pp. 221-226, 1994.
19) Matsumoto, M., Chen, X. and Shiraishi, N.: "Buffeting Analysis of Long-Span Bridges by Considering Aeroelastic Coupling", *Proc. of 13th Symposium of JAWE*, pp. 227-232, 1994.
20) Katsuchi, H., Kitagawa, M., Kanazaki, T., Toriumi, R. and Otani, Y.: "A Study of Effect of Spatial Correlation on Buffeting Response of Long-Span Bridges", *Proc. of 50th Annual Conference of JSCE*, Vol. I, pp. 1468-1469, 1995.